Enhancing residual-based techniques with shape reconstruction features in Electrical Impedance Tomography

Bastian Harrach[†] **and Mach Nguyet Minh**[†]

† Department of Mathematics, Goethe University Frankfurt, Germany

E-mail: `harrach@math.uni-frankfurt.de, mach@math.uni-frankfurt.de`

Abstract. In electrical impedance tomography, algorithms based on minimizing a linearized residual functional have been widely used due to their flexibility and good performance in practice. However, no rigorous convergence results have been available in the literature yet, and reconstructions tend to contain ringing artifacts. In this work, we shall minimize the linearized residual functional under a linear constraint defined by a monotonicity test, which plays a role of a special regularizer. Global convergence is then established to guarantee that this method is stable under the effects of noise. Moreover, numerical results show that this method yields good shape reconstructions under high levels of noise without appearance of artifacts.

AMS classification scheme numbers: 35R30, 35J25

1. Introduction

Electrical impedance tomography (EIT) is a non-invasive imaging technique which aims to reconstruct the electric conductivity inside a reference subject from the knowledge of the current and voltage measurements on the boundary of the subject. Typically, a finite number of electrodes are attached to the boundary of the reference subject, then small currents are applied to some or all of the electrodes and the resulting electric voltages are measured from the other electrodes. Compared with computerized X-ray tomography, EIT is less costly and requires no ionizing radiation; hence, it qualifies for many clinical applications including lung ventilation (e.g. [7]), brain imaging (e.g. [26]), breast cancer diagnosis (e.g. [5]), etc. On the other hand, EIT can also be used for nonclinical purposes such as determining the location of mineral deposits (e.g. [21]), describing soil structure (e.g. [28]), identifying cracks in non-destructive testing (e.g. [17]) and so on.

The inverse problem of reconstructing the conductivity from voltage-current-measurements is known to be highly ill-posed and nonlinear, and the reconstructions suffer from an enormous sensitivity to modeling and measurement errors. To reduce modeling errors, one usually concentrates on reconstructing a conductivity change with respect to some known reference conductivity. Then, the most natural approach is to parametrize the support of the conductivity change and determine these parameters by an iterative, nonlinear inverse problems solver. This iterative method yields good reconstructions for a given good initial guess; however, it requires expensive computations and has no convergence results. Non-iterative methods such as Factorization Method ([22, 11]) and Monotonicity-based Method ([24, 13]), on the other hand, are rigorously justified, allow fast implementation and require no initial guess. However, the reconstructions tend to be rather sensitive to measurement errors.

In clinical studies, one usually starts by linearizing the EIT problem around a known reference conductivity. The resulting linearization problem can be regularized in various ways, for example, the authors in [4] considered the minimization problem of a linearized residual functional with some regularization term, which is similar to the standard Tikhonov regularization method. The algorithm proposed in [4] is fast and simple. However, no convergence proofs are available so far.

Our new method is also based on minimizing the linearized residual functional. However, instead of adding a regularization term, we employ one linear constraint defined by the monotonicity test [13, Theorem 4.1]. Global convergence of the shape reconstructions is then proved and numerical results show that this method provides good shape reconstructions even under high levels of noise. To the authors' knowledge, this is the first reconstruction method based on minimizing the residual which has a rigorous global convergence property. For the question of globally convergent algorithms for other classes of inverse problems, see for example [25].

The paper is organized as follows. Section 2 presents some preliminaries and notations. In section 3, we state and prove our theoretical results. Section 4 shows the numerical experiments and we conclude our paper with a brief discussion in section 5.

2. Preliminaries and notations

We consider a bounded domain Ω in $\mathbb{R}^n, n \geq 2$, with smooth boundary $\partial\Omega$ and outer normal vector ν. We assume that Ω is isotropic so that the electric conductivity $\sigma : \Omega \to \mathbb{R}$ is a scalar function, and that σ is bounded and strictly positive. Inside Ω, the electric potential $u : \Omega \to \mathbb{R}$ is governed by the so-called *conductivity equation*. On the boundary of Ω, it satisfies the *Neumann condition*:

$$\nabla \cdot \sigma \nabla u = 0 \ \text{ in } \Omega, \quad \sigma \partial_\nu u = g \ \text{ on } \partial\Omega. \tag{1}$$

For the sake of simplicity, we shall follow the *Continuum Model*, which assumes that there are no electrodes and that the injected currents $g : \partial\Omega \to \mathbb{R}$ are applied over all $\partial\Omega$. The electric voltages, in this case, can be measured at every point of the boundary $\partial\Omega$ and are denoted by $u|_{\partial\Omega}$.

The forward problem of (1) is to determine the potential u for given data σ and g. The existence of a variational solution $u \in H^1_\diamond(\Omega)$ for this Neumann boundary value problem is obtained due to Lax-Milgram Theorem, while the uniqueness (up to an additive constant) is straight-forward. The forward problem of (1) is well-posed in the sense that the potential u depends continuously on the Neumann data g. To guarantee that u is uniquely defined, one can require that the solution u has zero integral mean, i.e. $\int_{\partial\Omega} u \, \mathrm{d}s = 0$.

The unique solvability of the forward problem (1) guarantees the existence of the Neumann-to-Dirichlet (NtD) operator $\Lambda(\sigma)$, that maps each current g to the voltage measurement $u_g^\sigma|_{\partial\Omega}$ on the boundary:

$$\text{For each } \ \sigma \in L_+^\infty(\Omega),\ \Lambda(\sigma) : L_\diamond^2(\partial\Omega) \to L_\diamond^2(\partial\Omega) : g \mapsto u_g^\sigma|_{\partial\Omega}.$$

Here, $u_g^\sigma \in H_\diamond^1(\Omega)$ is the unique variational solution of the forward problem (1) corresponding to the conductivity σ and the boundary current g, and $u_g^\sigma|_{\partial\Omega}$ is understood as the trace of u_g^σ on the boundary $\partial\Omega$. $L_+^\infty(\Omega)$ is the subspace of $L^\infty(\Omega)$ with positive essential infima. $H_\diamond^1(\Omega)$ and $L_\diamond^2(\partial\Omega)$ denote the spaces of H^1- and L^2-functions with vanishing integral mean on $\partial\Omega$.

It is well-known that $\Lambda(\sigma)$ is a linear, bounded, compact, self-adjoint, positive operator from $L_\diamond^2(\partial\Omega)$ to $L_\diamond^2(\partial\Omega)$ (see for example [14, Chapter 5] for two dimensional-case). For each $g \in L_\diamond^2(\partial\Omega)$, the quadratic form associated with $\Lambda(\sigma)$ is:

$$\langle g, \Lambda(\sigma)g \rangle = \int_{\partial\Omega} g\Lambda(\sigma)g \ \mathrm{d}s = \int_\Omega \sigma |\nabla u_g^\sigma|^2 \ \mathrm{d}x.$$

The existence of the Fréchet derivative Λ' of the NtD operator Λ can be found, for example, in [18]. Given some direction $\kappa \in L^\infty(\Omega)$, the derivative $\Lambda'(\sigma)\kappa \in \mathcal{L}(L_\diamond^2(\partial\Omega))$ is associated to the quadratic form:

$$\langle g, (\Lambda'(\sigma)\kappa)g \rangle = -\int_\Omega \kappa |\nabla u_g^\sigma|^2 \ \mathrm{d}x.$$

The inverse problem of (1) is to determine the conductivity σ from the knowledge of the NtD operator $\Lambda(\sigma)$. Obviously, $\Lambda(\sigma)$ depends on σ nonlinearly, and like many other nonlinear inverse problems, this is an ill-posed problem. In fact, it is known that small amounts of noise or model errors can cause poor spatial resolution. The reader is referred to the book of Mueller and Siltanen [19] for more explanation about the nonlinearity and the ill-posedness of this inverse problem.

The uniqueness of solutions of the inverse problem (1) has been investigated for different classes of conductivities and dimensions right after the pioneer paper of Calderon [3] in 1980, for example, Kohn and Vogelius [16] for piecewise analytic conductivities, Sylvester and Uhlmann [23] for C^2-conductivities in dimension $n \geq 3$, Nachman [20] for $W^{2,p}$-conductivities in dimension $n = 2$, Astala and Päivärinta [1] for L^∞-conductivities in dimension $n = 2$.

In the next section, we shall propose one regularization scheme to construct an approximate solution and prove the stability in the presence of noise.

3. Theoretical results

In this work, we assume that the background conductivity $\sigma_0 \equiv 1$ and that the conductivity of the investigated subject is defined by $\sigma := 1+\gamma\chi_D$, where the measurable set D denotes the unknown inclusions. Assume moreover that $\gamma \in L^\infty_+(D)$ and that $\Omega \backslash D$ is connected. Our goal is to determine the inclusions' shape D from the knowledge of the NtD operators $\Lambda(\sigma)$ and $\Lambda(1)$.

3.1. Exact data

We start by describing our method for exact data. The idea of this method is inspired by a result of Seo and one of the authors in [12]. It is proved that, if κ is an exact solution of the linearized equation

$$\Lambda'(1)\kappa = \Lambda(\sigma) - \Lambda(1)$$

then the support of κ coincides with D. However, it is not clear in general that whether such an exact solution exists. In addition, one cannot get a similar result for noisy data. It is natural to ask whether minimizing the residual functional

$$r(\kappa) := \Lambda(\sigma) - \Lambda(1) - \Lambda'(1)\kappa$$

under appropriate regularization can yield a solution κ with correct support. In this work, we can prove that this can indeed be done. More precisely, denote by $\{g_1, \ldots, g_N\}$ the N given injected currents which are assumed to form an orthonormal subset of $L^2_\diamond(\partial\Omega)$, we can replace $r(\kappa)$ by the matrix $(\langle g_i, r(\kappa)g_j\rangle)_{i,j=1}^N$ and minimize this N-by-N matrix under the Frobenius norm:

$$\min_{\kappa\in\mathcal{A}\subset L^\infty(\Omega)} \|\mathbf{R}(\kappa)\|_F, \tag{2}$$

where $\mathbf{R}(\kappa)$ stands for the matrix $(\langle g_i, r(\kappa)g_j\rangle)_{i,j=1}^N$, $\|\cdot\|_F$ denotes the Frobenius norm and $\mathcal{A}$ is some admissible set of conductivity change κ. Since there is no hope to reconstruct the conductivity change at every point inside Ω from the knowledge of a finite number of measurements, it is reasonable to restrict $\mathcal{A}$ to the class of piecewise constant functions. More precisely, the admissible conductivity change κ is assumed to be constant on a fixed partition $\{P_k\}_{k=1}^P$ of the bounded domain Ω:

$$\kappa(x) = \sum_{k=1}^P a_k\chi_{P_k}(x),$$

where the a_k's are real constants and each P_k is assumed to be open, $\cup_{k=1}^P \overline{P}_k = \overline{\Omega}$, $\Omega \setminus P_k$ is connected and $P_k \cap P_l = \emptyset$ for $k \neq l$. Notice that, this partition is not unique, and any minimizer $\bar\kappa$ of (2) as well as any reconstruction shape (that is, the support of some minimizer $\bar\kappa$) depend heavily on the choice of this partition.

Remark 3.1. *It is well-known that $r(\kappa)$ is a linear, bounded, compact, self-adjoint operator from $L^2_\diamond(\partial\Omega)$ to $L^2_\diamond(\partial\Omega)$. Perhaps a reasonable choice of an appropriate norm to minimize $r(\kappa)$ is the operator norm. In fact, all of the following theoretical results* *remain true for the operator norm. The numerical results for the operator norm, on the other hand, can be easily obtained by considering the equivalent problem of minimizing the maximum eigenvalue of an approximate matrix of $r(\kappa)$, and then employing some* `MATLAB` *software for convex programming such as* **cvx**. *However, as we can see later, minimizing the residual functional $r(\kappa)$ under the operator norm does not yield good enough shape reconstructions. Another commonly used norm is the Hilbert-Schmidt norm. Nevertheless, we could not minimize $r(\kappa)$ under the Hilbert-Schmidt norm, since it is not clear that whether or not $r(\kappa)$ belongs to the class of Hilbert-Schmidt operators. The idea of using the Frobenius norm comes from the fact that in realistic models, one always applies a finite number of currents g on the boundary; and hence, there only a finite number of measurements $\Lambda(\sigma)g$ are known.*

Problem (2) is actually considered decades ago in clinical EIT such as [4]. Typically, one usually adds some regularization term into the minimization functional, similar to the standard Tikhonov regularization method. By this way, good shape reconstructions with real-time implementation can be obtained. However, no rigorous convergence results are established so far.

In the present paper, we do not follow the standard Tikhonow regularization method. Instead, we use one linear constraint defined by the monotonicity test [13] as a special regularizer.

A linear constraint defined by the monotonicity test

A lower bound for an admissible conductivity change κ is, in fact, due to the fact that $\sigma \geq 1$. An upper bound for κ, on the contrary, is numerically defined by the idea of the monotonicity test [13] as follows:

[13, Example 4.4] has proved that, for $\tilde{\sigma} = 1 + \chi_D$ and for every ball B

$$B \subseteq D \quad \text{if and only if} \quad \Lambda(1) + \frac{1}{2}\Lambda'(1)\chi_B \geq \Lambda(\tilde{\sigma}).$$

We will show in the proof of Lemma 3.4 that for any real constant $\mathbf{a}$ satisfying $0 < \mathbf{a} \leq 1 - \frac{1}{1+\inf_D \gamma}$, it holds that

(i) If $P_k \subseteq D$ then $\Lambda(1) - \Lambda(\sigma) + \alpha\Lambda'(1)\chi_{P_k} \geq 0$ in quadratic sense for (at least) all $\alpha \in [0, \mathbf{a}]$.

(ii) If $P_k \not\subseteq D$ then $\Lambda(1) - \Lambda(\sigma) + \alpha\Lambda'(1)\chi_{P_k} \ngeq 0$ in quadratic sense for all $\alpha > 0$.

For each pixel P_k, the biggest coefficient β_k such that

$$\Lambda(1) - \Lambda(\sigma) + \alpha\Lambda'(1)\chi_{P_k} \geq 0 \quad \forall \alpha \in [0, \beta_k] \tag{3}$$

is then satisfies

- $\beta_k \geq \mathbf{a} > 0$ if $P_k \subseteq D$.
- $\beta_k = 0$ if $P_k \not\subseteq D$.

This motivates the constraint $0 \leq \kappa \leq \beta_k$ on each pixel P_k. Note that β_k is allowed to be ∞. Our following theory, therefore, requires to use a stronger upper bound $\min(\mathbf{a}, \beta_k)$. Since $\mathbf{a}$ is usually smaller than the true contrast γ, this seems "over-constrained", but we will show that the minimizer of this over-constrained problem posseses the correct support. Thus, we can define the admissible set $\mathcal{A}$ as follows:

$$\mathcal{A} := \left\{ \kappa \in L^\infty(\Omega) \ : \ \kappa = \sum_{k=1}^{P} a_k \chi_{P_k}, a_k \in \mathbb{R}, 0 \le a_k \le \min(\mathbf{a}, \beta_k) \right\}.$$

Here comes our main result.

Theorem 3.2. *Consider the minimization problem*

$$\min_{\kappa \in \mathcal{A}} \|\mathbf{R}(\kappa)\|_F. \tag{4}$$

The following statements hold true:

(i) Problem (4) admits a unique minimizer $\hat{\kappa}$.

(ii) $\operatorname{supp} \hat{\kappa}$ *and D agree up to the pixel partition, i.e. for any pixel P_k*

$$P_k \subset \operatorname{supp} \hat{\kappa} \ \textit{ if and only if } \ P_k \subset D.$$

Moreover, $\hat{\kappa} = \sum_{k=1}^{P} \min(\mathbf{a}, \beta_k) \chi_{P_k}$.

Remark 3.3. *[18, Theorem 4.3] has proved that $\Lambda'(1)$ is injective if there are enough boundary currents (that is, if N is sufficiently large). In that case, it is obvious to see that $\mathbf{R}(\kappa)$ is also injective. This fact together with the fact that the square Frobenius norm is strictly convex imply $\kappa \mapsto \|\mathbf{R}(\kappa)\|_F^2$ is strictly convex.*

Before proving Theorem 3.2, we need the following lemmas.

Lemma 3.4. *For any pixel P_k, $P_k \subseteq D$ if and only if $\beta_k > 0$.*

One special case of Lemma 3.4 has been proved in [13, Example 4.4]. We have slightly modified the proof there to fit with our notations and settings.

Proof of Lemma 3.4. **Step 1:** We shall check that, $P_k \subseteq D$ implies $\beta_k > 0$. Indeed, employing the following monotonicity principle (see e.g. [13, Lemma 3.1]):

$$\langle g, (\Lambda(\sigma_2) - \Lambda(\sigma_1))g \rangle \ge \int_\Omega \frac{\sigma_2}{\sigma_1}(\sigma_1 - \sigma_2)|\nabla u_2|^2 \,\mathrm{d}x,$$

it is not hard to see that for all pixels P_k, for all $\alpha \in [0, \mathbf{a}]$ and all $g \in L^2_\diamond(\partial\Omega)$:

$$\begin{aligned}\langle g, (\Lambda(\sigma) - \Lambda(1) - \Lambda'(1)\alpha\chi_{P_k})g \rangle &\le -\int_\Omega \left(1 - \frac{1}{\sigma}\right) |\nabla u_g^0|^2 \,\mathrm{d}x + \int_\Omega \alpha \chi_{P_k} |\nabla u_g^0|^2 \le \\ &\le -\int_D \left(1 - \frac{1}{\sigma}\right) |\nabla u_g^0|^2 \,\mathrm{d}x + \int_{P_k} \mathbf{a}\, |\nabla u_g^0|^2 \,\mathrm{d}x \le 0.\end{aligned}$$

Here u_g^0 is the unique solution of the forward problem (1) when the conductivity is chosen to be 1. The last inequality holds due to the fact that $\mathbf{a} \le 1 - \frac{1}{1+\inf_D \gamma}$ and that P_k lies inside D.

Step 2: If $\beta_k > 0$, we will show that $P_k \subseteq D$ by contradiction: Assume that $\beta_k > 0$ and $P_k \nsubseteq D$. By the following monotonicity principle [13, Lemma 3.1]:

$$\Lambda(\sigma_1) - \Lambda(\sigma_2) \ge \Lambda'(\sigma_2)(\sigma_1 - \sigma_2),$$

we can write

$$0 \geq \Lambda(\sigma) - \Lambda(1) - \Lambda'(1)\beta_k\chi_{P_k} \geq \Lambda'(1)(\sigma - 1) - \Lambda'(1)\beta_k\chi_{P_k}.$$

Thus, for all $g \in L^2_\diamond(\partial\Omega)$:

$$\int_{P_k} \beta_k |\nabla u^0_g|^2 \,\mathrm{d}x \leq \int_\Omega (\sigma - 1)|\nabla u^0_g|^2 \,\mathrm{d}x \leq \int_D C|\nabla u^0_g|^2 \,\mathrm{d}x \tag{5}$$

with some positive constant C.

On the other hand, applying localized potential (see e.g. [13, Theorem 3.6] and [8] for the origin of this idea), we can find a sequence $\{g_m\} \subset L^2_\diamond(\partial\Omega)$ such that the solutions $\{u^0_m\} \subset H^1_\diamond(\Omega)$ of the forward problem (1) (when the conductivity is chosen to be 1 and boundary currents $g = g_m$) fulfill

$$\lim_{m\to\infty} \int_{P_k} |\nabla u^0_m|^2 \,\mathrm{d}x = \infty, \quad \text{and} \quad \lim_{m\to\infty} \int_D |\nabla u^0_m|^2 \,\mathrm{d}x = 0.$$

This contradicts (5). □

Lemma 3.5. *For all pixels P_k, denote by $\mathbf{S}_k$ the matrix $(-\langle g_i, \Lambda'(1)\chi_{P_k} g_j\rangle)_{i,j=1}^N$. Then $\mathbf{S}_k$ is a positive definite matrix.*

Proof of Lemma 3.5. For all $\mathrm{x} = (x_1, \ldots, x_N) \in \mathbb{R}^N$, we have

$$\mathrm{x}^\top \mathbf{S}_k \,\mathrm{x} = -\sum_{i,j=1}^N x_i x_j \langle g_i, \Lambda'(1)\chi_{P_k} g_j\rangle = -\langle g, \Lambda'(1)\chi_{P_k} g\rangle = \int_{P_k} |\nabla u^0_g|^2 \,\mathrm{d}x \geq 0,$$

where $g = \sum_{i=1}^N x_i g_i$. This means that $\mathbf{S}_k$ is a positive semi-definite symmetric matrix in $\mathbb{R}^{N\times N}$. We shall prove that $\mathbf{S}_k$ is, in fact, a positive definite matrix by showing that

$$\int_{P_k} |\nabla u^0_g|^2 \,\mathrm{d}x > 0 \quad \text{for all } \; g \in L^2_\diamond(\partial\Omega), \; \|g\|_{L^2_\diamond(\partial\Omega)} \neq 0. \tag{6}$$

Assuming, by contradiction, that there exists $\bar{g} \in L^2_\diamond(\partial\Omega), \|\bar{g}\|_{L^2_\diamond(\partial\Omega)} \neq 0$ such that

$$\int_{P_k} |\nabla u^0_{\bar{g}}|^2 \,\mathrm{d}x = 0.$$

Since P_k is open, there exists an open ball $B \subseteq P_k$. It holds that $u^0_{\bar{g}} = c$ a.e. B, where c is some real constant. This fact can be obtained in many different ways, for example, by the Poincaré's inequality.

On the other hand, $u(x) = c$ is a solution of the forward problem (1) with conductivity 1 and homogeneous Neumann boundary data. Therefore, $u^0_{\bar{g}} - c$ is a solution of (1) when the conductivity is 1 and the Neumann boundary is $\bar{g}$. Moreover, we have proved that $u^0_{\bar{g}} - c = 0$ a.e. in an open ball $B \subset \Omega$, the unique continuation principle implies that $u^0_{\bar{g}} - c = 0$ a.e. Ω, and hence $\bar{g} = 0$ a.e. $\partial\Omega$. This contradiction implies that (6) holds. □

Now we are in the position to prove our main result.

Proof of Theorem 3.2. **(i)** Existence of minimizer: Since the functional

$$\kappa \mapsto \|\mathbf{R}(\kappa)\|_F^2 := \sum_{i,j=1}^{N} \langle g_i, r(\kappa) g_j \rangle^2$$

is continuous, it admits a minimizer in the compact set $\mathcal{A}$. Uniqueness obviously follows when we have proven (ii).

(ii) Step 1: Denote by $\chi_i := \chi_{P_i}$. We shall check that, for all $\kappa = \sum_{k=1}^{P} \alpha_k \chi_k$ satisfying $0 \le \alpha_k \le \min(\mathbf{a}, \beta_k)$, it holds that $r(\kappa) \le 0$ in quadratic sense.

Notice that $\mathbf{a} \le 1 - \frac{1}{\sigma}$. In the same manner as the proof of Lemma 3.4, we can write

$$\langle g, (\Lambda(\sigma) - \Lambda(1) - \Lambda'(1)\kappa) g \rangle \le - \int_D \mathbf{a} |\nabla u_g^0|^2 \, \mathrm{d}x + \sum_{k=1}^{P} \int_{P_k} \alpha_k |\nabla u_g^0|^2 \, \mathrm{d}x$$

for any $g \in L^2_\diamond(\partial\Omega)$. By Lemma 3.4, if $\alpha_k > 0$ then $P_k \subseteq D$. Taking into account that $\alpha_k \le \mathbf{a}$ and that $P_i \cap P_j \neq \emptyset$ for $i \neq j$, we get that $\langle g, r(\kappa) g \rangle \le 0$ for any $g \in L^2_\diamond(\partial\Omega)$.

Step 2: Let $\hat{\kappa} = \sum_{k=1}^{P} \hat{\alpha}_k \chi_k$ be a minimizer of (4). We prove that $\mathrm{supp}\hat{\kappa} \subseteq D$.

Indeed, if $\hat{\alpha}_k > 0$, it follows from Step 1 that

$$\Lambda(\sigma) - \Lambda(1) - \Lambda'(1)\alpha_k \chi_k \le \Lambda(\sigma) - \Lambda(1) - \Lambda'(1)\hat{\kappa} \le 0.$$

Thanks to Lemma 3.4, we have $P_k \subseteq D$.

Step 3: If $\hat{\kappa} = \sum_{k=1}^{P} \hat{\alpha}_k \chi_k$ be a minimizer of (4), then $\hat{\kappa} = \sum_{k=1}^{P} \min(\mathbf{a}, \beta_k) \chi_k$.

Indeed, it holds that $\hat{\kappa} \le \sum_{k=1}^{P} \min(\mathbf{a}, \beta_k) \chi_k$. If there exists a pixel P_k such that $\hat{\kappa}(x) < \min\{\mathbf{a}, \beta_k\}$ in P_k, we can choose $h > 0$ such that $\hat{\kappa} + h\chi_k = \min(\mathbf{a}, \beta_k)$ in P_k. We will show that

$$\|\mathbf{R}(\hat{\kappa} + h\chi_k)\|_F < \|\mathbf{R}(\hat{\kappa})\|_F \tag{7}$$

which contradicts the minimality of $\hat{\kappa}$.

Let $\lambda_1(\hat{\kappa}) \ge \lambda_2(\hat{\kappa}) \ge \ldots \ge \lambda_N(\hat{\kappa})$ be N eigenvalues of $\mathbf{R}(\hat{\kappa})$ and $\lambda_1(\hat{\kappa} + h\chi_k) \ge \lambda_2(\hat{\kappa} + h\chi_k) \ge \ldots \ge \lambda_N(\hat{\kappa} + h\chi_k)$ be N eigenvalues of $\mathbf{R}(\hat{\kappa} + h\chi_k)$. Since $\mathbf{R}(\hat{\kappa})$ and $\mathbf{R}(\hat{\kappa} + h\chi_k)$ are both symmetric, all of their eigenvalues are real. By the definition of the Frobenius norm, we get

$$\begin{aligned} \|\mathbf{R}(\hat{\kappa} + h\chi_k)\|_F^2 - \|\mathbf{R}(\hat{\kappa})\|_F^2 &= \sum_{i=1}^{N} |\lambda_i(\hat{\kappa} + h\chi_k)|^2 - \sum_{i=1}^{N} |\lambda_i(\hat{\kappa})|^2 = \\ &= \sum_{i=1}^{N} \left(\lambda_i(\hat{\kappa} + h\chi_k) + \lambda_i(\hat{\kappa})\right) \cdot \left(\lambda_i(\hat{\kappa} + h\chi_k) - \lambda_i(\hat{\kappa})\right). \end{aligned} \tag{8}$$

Thanks to Step 1, $r(\hat{\kappa}) \le 0$ and $r(\hat{\kappa} + h\chi_k) \le 0$ in the quadratic sense. Thus, for all $\mathrm{x} = (x_1, \ldots, x_N) \in \mathbb{R}^N$, we have

$$\mathrm{x}^\top \mathbf{R}(\hat{\kappa})\, \mathrm{x} = \sum_{i,j=1}^{N} x_i x_j \langle g_i, r(\hat{\kappa}) g_j \rangle = \langle g, r(\hat{\kappa}) g \rangle \le 0,$$

where $g = \sum_{i=1}^{N} x_i g_i$. This means that $-\mathbf{R}(\hat{\kappa})$ is a positive semi-definite symmetric matrix in $\mathbb{R}^{N\times N}$. It is well-known that all eigenvalues of a positive semi-definite symmetric matrix should be non-negative. Thus,

$$\lambda_i(\hat{\kappa}) \leq 0 \quad \text{for all} \quad i \in \{1, \ldots, N\}. \tag{9}$$

In the same manner, $-\mathbf{R}(\hat{\kappa} + h\chi_k)$ is also a positive semi-definite symmetric matrix. Hence,

$$\lambda_i(\hat{\kappa} + h\chi_k) \leq 0 \quad \text{for all} \quad i \in \{1, \ldots, N\}. \tag{10}$$

On the other hand, Lemma 3.5 claims that $\mathbf{S}_k$ is a positive definite matrix. Thus, all N eigenvalues $\lambda_1(\mathbf{S}_k) \geq \ldots \geq \lambda_N(\mathbf{S}_k)$ of $\mathbf{S}_k$ are positive. Since

$$\mathbf{R}(\hat{\kappa} + h\chi_k) = \mathbf{R}(\hat{\kappa}) + h\mathbf{S}_k.$$

and the matrices $\mathbf{R}(\hat{\kappa} + h\chi_k), \mathbf{R}(\hat{\kappa})$ and $\mathbf{S}_k$ are all symmetric, we can apply Weyl's Inequalities [2, Theorem III.2.1] to get

$$\lambda_i(\hat{\kappa} + h\chi_k) \geq \lambda_i(\hat{\kappa}) + h\lambda_N(\mathbf{S}_k) > \lambda_i(\hat{\kappa}) \quad \text{for all} \quad i \in \{1, \ldots, N\}. \tag{11}$$

In summary, (8), (9), (10) and (11) imply (7). This ends the proof of Step 3.

Step 4: If $P_k \subseteq D$, then $P_k \subseteq \mathrm{supp}\hat{\kappa}$. Indeed, since $\hat{\kappa}$ is a minimizer of (4), Step 3 implies that $\hat{\kappa} = \sum_{k=1}^{P} \min(\mathbf{a}, \beta_k)\chi_k$. Since $P_k \subseteq D$, it follows from Lemma 3.4 that $\min(\mathbf{a}, \beta_k) > 0$. Thus, $P_k \subseteq \mathrm{supp}\hat{\kappa}$.

In conclusion, problem (4) admits a unique minimizer $\hat{\kappa} = \sum_{k=1}^{P} \min(\mathbf{a}, \beta_k)\chi_k$. This minimizer fulfills

$$\hat{\kappa} = \begin{cases} \mathbf{a} & \text{in } P_k, \quad \text{if } P_k \text{ lies inside } D, \\ 0 & \text{in } P_k, \quad \text{if } P_k \text{ does not lie inside } D. \end{cases}$$

□

3.2. Convergence for noisy data

In the presence of noise, assume that $\delta\%$ is the noise level. Similarly as above, we denote by $\mathbf{R}^\delta(\kappa)$ the N-by-N matrix $\left(\langle g_i, r^\delta(\kappa) g_j\rangle\right)_{i,j=1}^{N}$, where the residual for noisy data now reads

$$r^\delta(\kappa) := \Lambda^\delta(\sigma) - \Lambda(1) - \Lambda'(1)\kappa,$$

and the error is bounded from above by δ in the operator norm, i.e.

$$\|\Lambda^\delta(\sigma) - \Lambda(\sigma)\|_{\mathcal{L}(L^2_\diamond(\partial\Omega))} \leq \delta.$$

When we replace the exact data $\Lambda(\sigma)$ by the noisy data $\Lambda^\delta(\sigma)$, we have to change the definition of the biggest coefficient β_k, too. To this end, we need the following lemma:

Lemma 3.6. *For any bounded linear operator T on a real Hilbert space H:*

(i) (Square Root Lemma) If T is positive, i.e. T is self-adjoint and $\langle x, Tx\rangle \geq 0$ for all $x \in H$, then there exists a unique bounded linear positive operator U on H such that $U^2 = T$. Moreover, U commutes with every bounded linear operator which commutes with T. We call U the positive square root of T and denote by $U = \sqrt{T}$.

(ii) (Absolute value of a bounded linear operator) The modulus of T

$$|T| := \sqrt{T^*T}$$

is a positive operator, where T^* is the adjoint operator of T. Moreover, $|T|$ commutes with every bounded linear operator which commutes with T^*T.

(iii) (Positive decomposition) If T is self-adjoint, then there exists a unique pair of bounded positive operators T_+ and T_- such that $T = T_+ - T_-$, $T_+T_- = 0$, T_+ and T_- commute with each other and with T. Moreover, $|T| = T_+ + T_-$.

(iv) If T is positive, then $|T| = T$.

(v) If T is self-adjoint, then $T \leq |T|$ in quadratic sense.

(vi) For any bounded linear operators A, B on a real Hilbert space H:

$$\||A| - |B|\|^2_{\mathcal{L}(H)} \leq \left(\|A\|_{\mathcal{L}(H)} + \|B\|_{\mathcal{L}(H)}\right) \|A - B\|_{\mathcal{L}(H)}. \tag{12}$$

Consequently, the absolute value of operators is continuous w.r.t. the operator norm.

Proof of Lemma 3.6. (i) This famous fact can be proved either by means of classical functional analysis (see, for example, [27, Appendix]) or by using C^*-algebra techniques ([6, Proposition 4.33]).

(ii) For all $x \in H$, it holds that

$$\langle x, T^*Tx\rangle = \langle Tx, Tx\rangle \geq 0 \quad \text{and} \quad \langle x, T^*Tx\rangle = \langle Tx, Tx\rangle = \langle T^*Tx, x\rangle .$$

Hence, T^*T is a positive operator. Thanks to (i), T^*T has a unique positive square root $\sqrt{T^*T}$, which commutes with every bounded linear operator commuting with T^*T.

(iii) We shall prove this fact by using techniques in C^*-algebra. Indeed, since T is self-adjoint, it is normal. Hence, the Gelfand map Γ establishes a $*$-isometric isomorphism between the space of continuous functions on $\sigma(T)$ (here $\sigma(T)$ denotes the spectrum of T) and the C^*-algebra $\mathfrak{C}^*$ (see, e.g. [6, Theorem 2.31]). Define by

$$f_+(x) = \max(x, 0) \quad \text{and} \quad f_-(x) = -\min(x, 0),$$

then both f_+ and f_- are continuous positive functions on $\sigma(T)$. Thus, $T_+ := f_+(T) = \Gamma(f_+)$ and $T_- := f_-(T) = \Gamma(f_-)$ are well-defined positive operators on the space of bounded linear operators $\mathcal{B}(H)$. Moreover, T_+ and T_- commute with each other and with T. Since f_+ and f_- satisfy

$$f_+(x) - f_-(x) = x, \quad f_+(x) + f_-(x) = |x|, \quad f_+(x)f_-(x) = 0$$

for all x, it follows that the two positive operators T_+ and T_- satisfy

$$T_+ - T_- = T, \quad T_+ + T_- = |T|, \quad T_+T_- = 0.$$

On the other hand, we also have

$$\|T_+\|_{\mathcal{L}(H)} = \sup_{x\in\sigma(T)} |f_+(x)| \leq \sup_{x\in\sigma(T)} |x| = \|T\|_{\mathcal{L}(H)}.$$

By the same way, one can prove that T_- is also a bounded operator. It remains to show that the pair (T_+, T_-) is unique. Indeed, if $T = A - B$ where A, B are positive bounded operators satisfying $AB = 0$, then $T^2 = A^2 + B^2 = (A+B)^2$. Thus $A+B$ is the unique square root of T^2, i.e. $A + B = |T|$. Hence, $A = (|T| + T)/2 = T_+$ and $B = (|T| - T)/2 = T_-$. The uniqueness holds.

(iv) Since T is positive, it holds that $T^2 = T^*T$. Thanks to (i), T is a unique positive square roof of T^*T, i.e. $T = \sqrt{T^*T}$. On the other hand, by (ii), $\sqrt{T^*T} = |T|$. Thus, $T = |T|$.

(vi) First we prove that, for any linear, bounded, positive operators U, V on a real Hilbert space H, it holds that

$$\|U - V\|^2_{\mathcal{L}(H)} \leq \|U^2 - V^2\|_{\mathcal{L}(H)}. \tag{13}$$

The above inequality had been proved in [15, Theorem 1]. We shall recite the proof here for the reader's convenience.

Denote by $W := U - V$ then W is linear bounded self-adjoint operator on H. Hence

$$\|W\|_{\mathcal{L}(H)} = \sup_{\|g\|_H=1} |\langle g, Wg\rangle|.$$

Thus, we can find a sequence $\{g_n\} \subset H$ such that

$$\|g\|_H = 1 \quad \text{and} \quad |\langle g_n, Wg_n\rangle| \uparrow \|W\|_{\mathcal{L}(H)} \quad \text{as } n \to \infty.$$

Denote by $t := \|W\|_{\mathcal{L}(H)}$, we have

$$\begin{aligned}
\|U^2 - V^2\|_{\mathcal{L}(H)} &= \|UW + WV\|_{\mathcal{L}(H)} \geq |\langle g_n, (UW + WV)g_n\rangle| \\
&= |\langle g_n, U(W-t)g_n\rangle + \langle (W-t)g_n, Vg_n\rangle + t\,\langle g_n, (U+V)g_n\rangle| \\
&\geq t\,\langle g_n, (U+V)g_n\rangle - |\langle g_n, U(W-t)g_n\rangle| - |\langle (W-t)g_n, Vg_n\rangle|. \quad (14)
\end{aligned}$$

Since both U and V are positive operators, we have $U + V \geq \pm W$. Thus,

$$\langle g_n, (U+V)g_n\rangle \geq |\langle g_n, Wg_n\rangle| \quad \text{for all } n. \tag{15}$$

On the other hand, $Wg_n \to tg_n$ as $n \to \infty$ because

$$\begin{aligned}
\|Wg_n - tg_n\|^2_{\mathcal{L}(H)} &= \langle Wg_n - tg_n, Wg_n - tg_n\rangle = \|Wg_n\|^2 - 2t\,\langle g_n, Wg_n\rangle + t^2 \\
&\leq 2t^2 - 2t\,\langle g_n, Wg_n\rangle.
\end{aligned}$$

Combining (14), (15) and taking $n \to \infty$, we get (13).

Thanks to (13), for all bounded linear operators A and B we have

$$\begin{aligned}
\||A| - |B|\|^2_{\mathcal{L}(H)} &\leq \||A|^2 - |B|^2\|_{\mathcal{L}(H)} = \|A^*A - B^*B\|_{\mathcal{L}(H)} \\
&\leq \|A^*\|_{\mathcal{L}(H)}\|A - B\|_{\mathcal{L}(H)} + \|A^* - B^*\|_{\mathcal{L}(H)}\|B\|_{\mathcal{L}(H)} \\
&= \left(\|A\|_{\mathcal{L}(H)} + \|B\|_{\mathcal{L}(H)}\right)\|A - B\|_{\mathcal{L}(H)}.
\end{aligned}$$

□

Back to our issues, since $V := \Lambda(1) - \Lambda(\sigma)$ is a linear bounded positive operator, Lemma 3.6 yields that $|V| = V$. The monotonicity test (3) can be rewritten as

$$|V| + \alpha\Lambda'(1)\chi_{P_k} \geq 0 \quad \text{for all} \quad \alpha \in [0, \beta_k]. \tag{16}$$

When replacing the exact data $\Lambda(\sigma)$ by the noisy data $\Lambda^\delta(\sigma)$, the above inequality does not hold in general for all $P_k \subseteq D$. Indeed, since the operator in the left-hand side of (16) is compact, it has eigenvalues arbitrarily close to zero. A small noise will make these eigenvalues a little bit negative which can make the β_k defined in (16) zero everywhere. Hence, we replace the test (16) with

$$|V^\delta| + \alpha\Lambda'(1)\chi_k \geq -\delta I \tag{17}$$

where $V^\delta := \Lambda(1) - \Lambda^\delta(\sigma)$ and I is the identity operator from $L^2_\diamond(\partial\Omega)$ to $L^2_\diamond(\partial\Omega)$. Since we can always redefine the data V^δ by defining $V^\delta := (V^\delta + (V^\delta)^*)/2$, without loss of generality, we can assume that V^δ is self-adjoint.

We then define β_k^δ as the biggest coefficient such that inequality (17) holds for all $\alpha \in [0, \beta_k^\delta]$. We see that, $\min(\mathbf{a}, \beta_k^\delta)$ will still be $\mathbf{a}$ inside the inclusions but possibly a little bit larger than 0 outside. More precisely, we have the following lemma:

Lemma 3.7. *Assume that* $\|\Lambda^\delta(\sigma) - \Lambda(\sigma)\|_{\mathcal{L}(L^2_\diamond(\partial\Omega))} \leq \delta$, *then for every pixel* P_k, *it holds that* $\beta_k \leq \beta_k^\delta$ *for all* $\delta > 0$.

Proof of Lemma 3.7. It is sufficient to check that β_k satisfies (17). Indeed, since the operator $V - V^\delta$ is linear, bounded and self-adjoint, we have for all $\|g\|_{L^2_\diamond(\partial\Omega)} = 1$:

$$\left|\left\langle g, (V - V^\delta)g\right\rangle\right| \leq \|V - V^\delta\|_{\mathcal{L}(L^2_\diamond(\partial\Omega))} = \|\Lambda^\delta(\sigma) - \Lambda(\sigma)\|_{\mathcal{L}(L^2_\diamond(\partial\Omega))} \leq \delta.$$

Now for any $\tilde{g} \in L^2_\diamond(\partial\Omega)$, if $\|\tilde{g}\|_{L^2_\diamond(\partial\Omega)} \neq 0$, then

$$\left|\left\langle \tilde{g}, (V - V^\delta)\tilde{g}\right\rangle\right| = \|\tilde{g}\|^2 \left|\left\langle \frac{\tilde{g}}{\|\tilde{g}\|}, (V - V^\delta)\frac{\tilde{g}}{\|\tilde{g}\|}\right\rangle\right| \leq \delta\|\tilde{g}\|^2.$$

Thus, $V^\delta - V \geq -\delta I$ in quadratic sense. Besides, Lemma 3.6 implies $|V^\delta| \geq V^\delta$. Hence,

$$|V^\delta| + \beta_k\Lambda'(1)\chi_k \geq V^\delta + \beta_k\Lambda'(1)\chi_k = V + \beta_k\Lambda'(1)\chi_k + V^\delta - V \geq -\delta I.$$

□

As a consequence of Lemma 3.7, it holds that

1. If P_k lies inside D, then $\beta_k^\delta \geq a$.
2. If $\beta_k^\delta = 0$, then P_k does not lie inside D.

We end this section by proving the following stability result:

Theorem 3.8. *Consider the minimization problem*

$$\min_{\kappa \in \mathcal{A}^\delta} \|\mathbf{R}^\delta(\kappa)\|_F \tag{18}$$

where $\mathbf{R}^\delta(\kappa)$ *represents the* N*-by-*N *matrix* $\left(\langle g_i, r^\delta(\kappa) g_j\rangle\right)_{i,j=1}^N$*, and the admissible set for noisy data is defined by*

$$\mathcal{A}^\delta := \left\{ \kappa \in L^\infty(\Omega) : \kappa = \sum_{k=1}^{P} a_k \chi_{P_k},\ a_k \in \mathbb{R},\ 0 \le a_k \le \min(\mathbf{a}, \beta_k^\delta) \right\}.$$

The following statements hold true:

(i) Problem (18) admits a minimizer.

(ii) Let $\hat\kappa := \sum_{k=1}^{P} \min(\mathbf{a}, \beta_k)\chi_k$ *and* $\hat\kappa^\delta := \sum_{k=1}^{P} \hat a_k^\delta \chi_k$ *be minimizers of problems (4) and (18) respectively. Then* $\hat\kappa^\delta$ *pointwise converges to* $\hat\kappa$ *as* $\delta \to 0$.

Remark 3.9. *Same argument as Remark 3.3, we get the strict convexity of* $\kappa \mapsto \|\mathbf{R}^\delta(\kappa)\|_F^2$ *when the number* N *of boundary currents are sufficiently large. Since all minimizers of (18) minimize* $\|\mathbf{R}^\delta(\kappa)\|_F^2$*, it holds that (18) has a unique minimizer if* N *is sufficiently large.*

Proof of Theorem 3.8. **(i)** The existence of minimizers of (18) is obtained in the same manner as Theorem 3.2(i). Indeed, since the functional $\kappa \mapsto \|\mathbf{R}^\delta(\kappa)\|_F^2$ is continuous, (18) admits at least one minimizer in the compact set $\mathcal{A}^\delta$.

(ii) Step 1: Convergence of a subsequence of $\hat\kappa^\delta$

For any fixed k, the sequence $\{\hat a_k^\delta\}_{\delta>0}$ is bounded from below by 0 and from above by $\mathbf{a}$. By Weierstrass' Theorem, there exists a subsequence $(\hat a_1^{\delta_n}, \dots, \hat a_P^{\delta_n})$ converges to some limit $(a_1, \dots, a_P)$. Of course, $0 \le a_k \le \mathbf{a}$ for all $k = 1, \dots, P$.

Step 2: Upper bound of the limit

We shall check that $a_k \le \beta_k$ for all $k = 1, \dots, P$. Indeed, thanks to (12)

$$\begin{aligned}\||V^\delta| - |V|\|_{\mathcal{L}(L^2_\diamond(\partial\Omega))}^2 &\le \left(\|V^\delta\|_{\mathcal{L}(L^2_\diamond(\partial\Omega))} + \|V\|_{\mathcal{L}(L^2_\diamond(\partial\Omega))}\right) \|V^\delta - V\|_{\mathcal{L}(L^2_\diamond(\partial\Omega))} \\ &\le (2\|V\|_{\mathcal{L}(L^2_\diamond(\partial\Omega))} + \delta)\delta.\end{aligned}$$

Thus, $|V^\delta|$ converges to $|V|$ in the operator norm as $\delta \to 0$. Hence, for any fixed k,

$$|V| + a_k \Lambda'(1)\chi_k = \lim_{\delta_n \to 0} \left(|V^{\delta_n}| + \hat a_k^{\delta_n} \Lambda'(1)\chi_k\right)$$

in the operator norm. It is straight-forward to see that, for any $g \in L^2_\diamond(\partial\Omega)$

$$\langle g, (|V| + a_k \Lambda'(1)\chi_k) g\rangle = \lim_{\delta_n \to 0} \left\langle g, (|V^{\delta_n}| + \hat a_k^{\delta_n} \Lambda'(1)\chi_k) g\right\rangle \ge -\lim_{\delta_n \to 0} \langle g, \delta_n g\rangle = 0.$$

Step 3: Minimality of the limit

By Theorem 3.2 and Lemma 3.7, $\min(\mathbf{a}, \beta_k) \le \min(\mathbf{a}, \beta_k^\delta)$ for all $k = 1, \dots, P$. Thus, $\hat\kappa$ belongs to the admissible class of the minimization problem (18) for all $\delta > 0$. By the minimality of $\hat\kappa^\delta$, we get

$$\|\mathbf{R}^\delta(\hat\kappa^\delta)\|_F \le \|\mathbf{R}^\delta(\hat\kappa)\|_F. \tag{19}$$

Denote by $\kappa = \sum_{k=1}^{P} a_k \chi_k$, where a_k's are the limits obtained in Step 1. We have that

$$\|\mathbf{R}^{\delta_n}(\hat\kappa^{\delta_n})\|_F^2 = \sum_{i,j=1}^{N} \left\langle g_i, \left(-V^{\delta_n} - \sum_{k=1}^{P} \hat a_k^{\delta_n} \Lambda'(1)\chi_k\right) g_j \right\rangle^2$$

and

$$\|\mathbf{R}(\kappa)\|_F^2 = \sum_{i,j=1}^{N} \left\langle g_i, \left(-V - \sum_{k=1}^{P} a_k \Lambda'(1)\chi_k \right) g_j \right\rangle^2 .$$

Since V^δ converges to V in the operator norm, for all fixed $g \in L^2_\diamond(\partial\Omega)$, $V^\delta g$ converges to Vg in $L^2_\diamond(\partial\Omega)$. Taking into account of the fact that $\hat{a}_k^{\delta_n}$ converges to a_k for any $k \in \{1,\ldots,P\}$ as $\delta_n \to 0$, it is easy to check that $\|\mathbf{R}^{\delta_n}(\hat{\kappa}^{\delta_n})\|_F$ converges to $\|\mathbf{R}(\kappa)\|_F$ as $\delta_n \to 0$. In the same manner, we can show that $\|\mathbf{R}^{\delta_n}(\hat{\kappa})\|_F$ converges to $\|\mathbf{R}(\hat{\kappa})\|_F$. Thus, it follows from (19):

$$\|\mathbf{R}(\kappa)\|_F \leq \|\mathbf{R}(\hat{\kappa})\|_F.$$

Since κ belongs to the admissible class of problem (4), the above inequality implies that it is in fact a minimizer of (4). By the uniqueness of the minimizer, we obtain $\kappa = \hat{\kappa}$, that is $a_k = \min(\mathbf{a}, \beta_k)$.

Step 4: Convergence of the whole sequence $\hat{\kappa}^\delta$

We have proved so far that every subsequence of $(\hat{a}_1^\delta, \ldots, \hat{a}_P^\delta)$ has a convergent subsubsequence, that converges to the limit $l = (\min(\mathbf{a}, \beta_1), \ldots, \min(\mathbf{a}, \beta_P))$. This implies the convergence of the whole sequence $(\hat{a}_1^\delta, \ldots, \hat{a}_P^\delta)$ to l. This ends the proof of Theorem 3.8. □

4. Numerical results

We do the numerical experiment for the case Ω is the unit disk in $\mathbb{R}^2$ centered at the origin. We consider the injected currents g_i in the following orthonormal set of $L^2(\partial\Omega)$:

$$\left\{ \frac{1}{\sqrt{\pi}} \sin(j\phi), \frac{1}{\sqrt{\pi}} \cos(j\phi) \;\middle|\; j = 1, \ldots, N \right\},$$

here and in the following, we choose $N = 16$ and ϕ is an angle from the positive x-axis. We shall follow the notations in Section 3. Denote by $\mathbf{V}^\delta$ the matrix $(\langle g_i, V^\delta g_j \rangle)_{i,j=1}^N$. The minimization matrix $\mathbf{R}^\delta(\kappa)$ now reads

$$\mathbf{R}^\delta(\kappa) = \mathbf{V}^\delta + \sum_{k=1}^{P} a_k \mathbf{S}_k,$$

and we would like to find $(a_1, \ldots, a_P)$ satisfying the linear constraint $0 \leq a_k \leq \min(\mathbf{a}, \beta_k^\delta)$ so that $\|\mathbf{R}^\delta(\kappa)\|_F$ is minimized.

First, we shall collect the known data $\mathbf{V}^\delta$ and $\mathbf{S}_k$. Then we calculate β_k^δ, and finally, minimize $\mathbf{R}^\delta(\kappa)$.

4.1. Generating data

Notice that $\mathbf{V}^\delta$ is the difference between two matrices $(\langle g_i, \Lambda(1) g_j \rangle)_{i,j=1}^N$ and $(\langle g_i, \Lambda^\delta(\sigma) g_j \rangle)_{i,j=1}^N$. While $(\langle g_i, \Lambda(1) g_j \rangle)_{i,j=1}^N$ and $\mathbf{S}_k$ can be computed directly, $(\langle g_i, \Lambda^\delta(\sigma) g_j \rangle)_{i,j=1}^N$ is obtained with the help of `COMSOL`, one commercial finite element software.

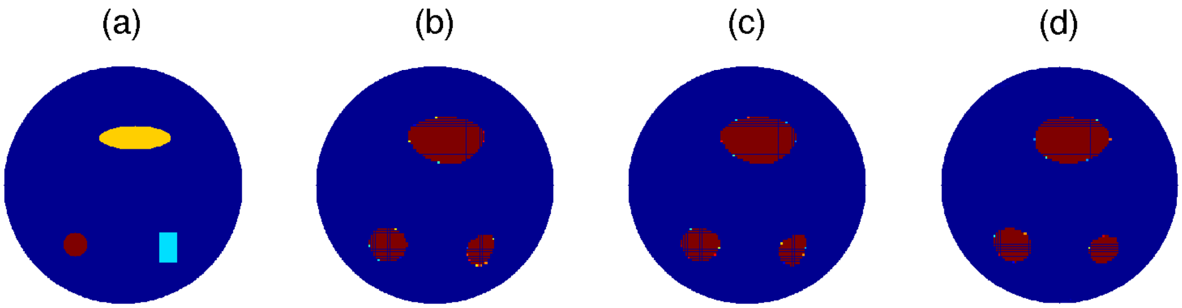

Figure 1. Reconstruction of conductivity change under a linear constraint defined by the monotonicity test: (a) true distribution of conductivity change; (b) $\frac{\delta}{\|\mathbf{V}\|_F} = 0.1\%$; (c) $\frac{\delta}{\|\mathbf{V}\|_F} = 1\%$; (d) $\frac{\delta}{\|\mathbf{V}\|_F} = 5\%$.

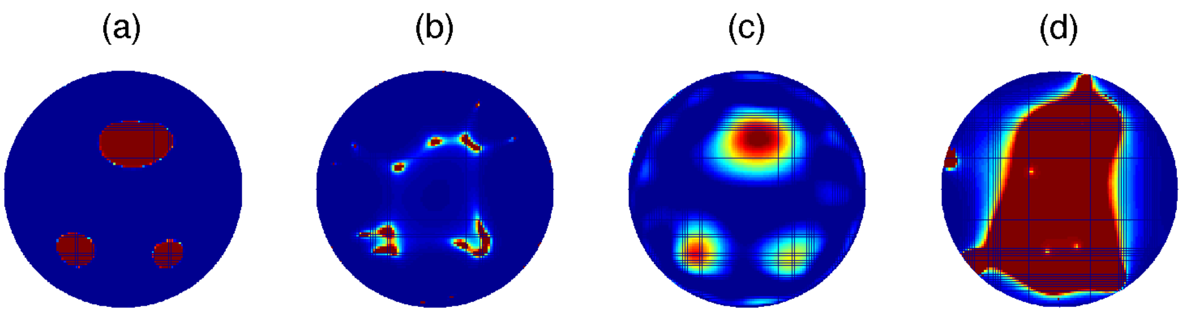

Figure 2. Reconstruction of conductivity change with 5% relative noise: (a) constraint $0 \leq \kappa \leq a$; (b) constraint $0 \leq \kappa \leq \sum_{k=1}^{P} \beta_k^\delta \chi_k$; (c) without constraint, regularization term $10^{-5}\|x\|_2$; (d) in the operator norm, constraint $0 \leq \kappa \leq \sum_{k=1}^{P} \min(\mathbf{a}, \beta_k^\delta)$.

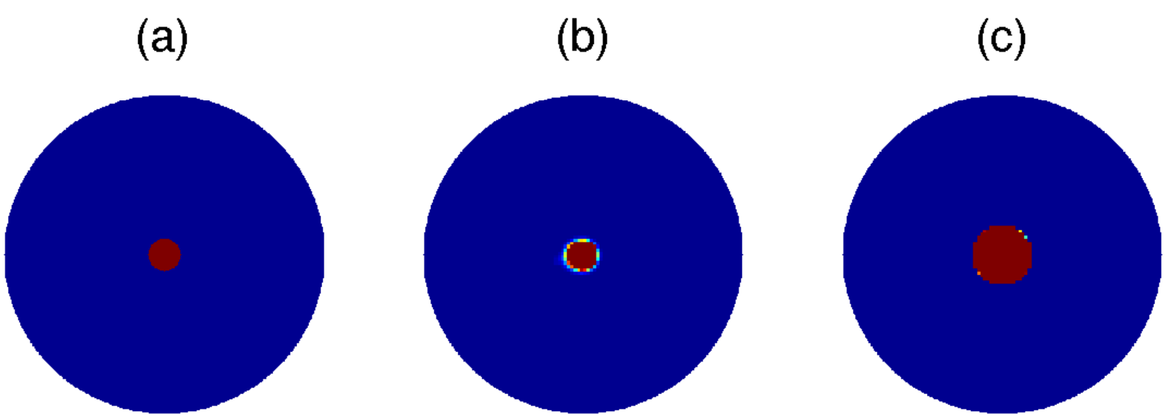

Figure 3. Reconstruction of conductivity change with 10^{-11} relative noise: (a) true distribution of conductivity change; (b) constraint $0 \leq \kappa \leq \sum_{k=1}^{P} \min(a, \beta_k^\delta)\chi_k$; (c) constraint $0 \leq \kappa \leq a$.

When the conductivity is chosen to be 1, the forward problem (1) becomes the Laplace equation with Neumann boundary condition g_j, and admits a unique solution

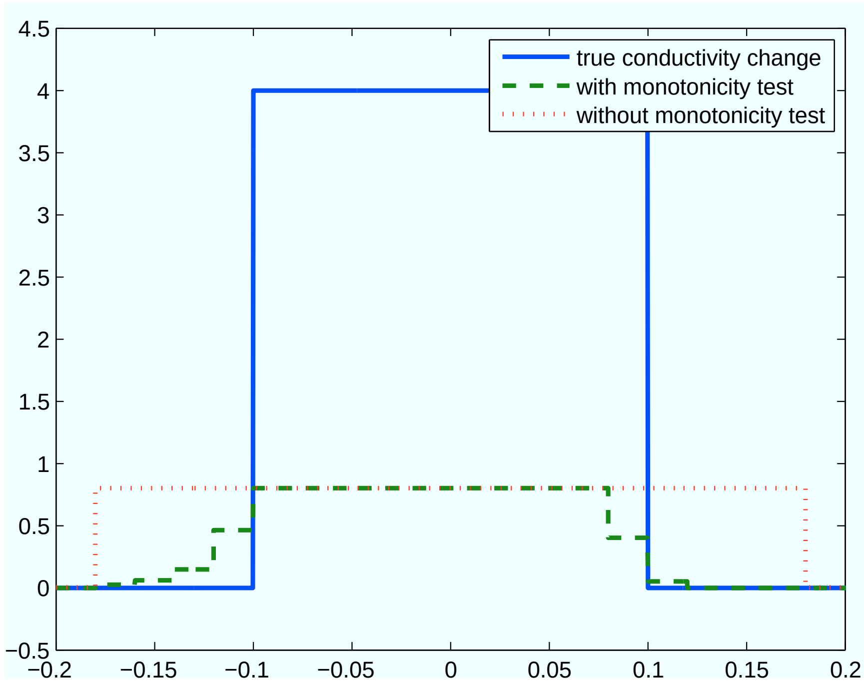

Figure 4. Cut of Figure 3 through the x-axis.

on the unit disk:

$$u_j^0 = \begin{cases} \dfrac{1}{j\sqrt{\pi}} \sin(j\varphi) r^j, & \text{if } g_j = \frac{1}{\sqrt{\pi}} \sin(j\varphi), \\ \dfrac{1}{j\sqrt{\pi}} \cos(j\varphi) r^j, & \text{if } g_j = \frac{1}{\sqrt{\pi}} \cos(j\varphi), \end{cases} \tag{20}$$

here the pair (r, ϕ) forms the polar coordinates with respect to the center of Ω. $(\langle g_i, \Lambda(1) g_j \rangle)_{i,j=1}^N$ and $\mathbf{S}_k$ are uniquely defined via:

$$\langle g_i, \Lambda(1) g_j \rangle = \int_{\partial\Omega} g_i u_j^0 \quad \text{and} \quad (\mathbf{S}_k)_{i,j} = -\langle g_i, \Lambda'(1) \chi_k g_j \rangle = \int_{P_k} \nabla u_i^0 \cdot \nabla u_j^0.$$

To calculate $(\langle g_i, \Lambda^\delta(\sigma) g_j \rangle)_{i,j=1}^N$, we follow the method suggested in [9], which first uses `COMSOL` to compute $\mathbf{V}$, the exact version of $\mathbf{V}^\delta$. We have

$$\mathbf{V}_{i,j} = \langle g_i, (\Lambda(1) - \Lambda(\sigma)) g_j \rangle = \int_{\partial\Omega} g_i (u_j^0 - u_j),$$

where u_j is the unique solution of (1) for conductivity σ and boundary current g_j. Denote by d_j the difference $u_j^0 - u_j$, then d_j satisfies the following system

$$\begin{aligned} \nabla \cdot \left(\sigma \nabla d_j - (\sigma - 1) \nabla u_j^0 \right) &= 0 \quad \text{in } \Omega, \\ \left(\sigma \nabla d_j - (\sigma - 1) \nabla u_j^0 \right) \cdot \nu &= 0 \quad \text{on } \partial\Omega. \end{aligned} \tag{21}$$

This system can be solve by using the Coefficient Form PDE model built by `COMSOL`. Notice that, we have to add the constraint $\int_{\partial\Omega} d_j = 0$ in order to guarantee the uniqueness of solution of (21).

Under $\delta\%$ of absolute noise, the noisy data $\mathbf{V}^\delta$ can be obtained from $\mathbf{V}$ by

$$\mathbf{V}^\delta := \mathbf{V} + \frac{\mathbf{E}}{\|\mathbf{E}\|_F}\delta\%,$$

here $\mathbf{E}$ is a random matrix in $\mathbb{R}^{N\times N}$ with uniformly distributed entries between -1 and 1. The Hermitian property of $\mathbf{V}^\delta$ follows by redefining $\mathbf{V}^\delta := ((\mathbf{V}^\delta)^* + \mathbf{V}^\delta)/2$.

4.2. Finding β_k^δ

To calculate β_k^δ, we follow the argument in [10]. First, we rewrite the formula (17) for matrices $\mathbf{V}^\delta$ and $\mathbf{S}_k$:

$$-\alpha\mathbf{S}_k \geq -\delta\mathbf{I} - |\mathbf{V}^\delta| \quad \text{for all} \quad \alpha \in [0, \beta_k^\delta]. \tag{22}$$

where the modulus $|\mathbf{V}^\delta| := \sqrt{(\mathbf{V}^\delta)^*\mathbf{V}^\delta}$ in this case is called the absolute value of matrices.

Since $\delta\mathbf{I} + |\mathbf{V}^\delta|$ is Hermitian positive-definite, the Cholesky decomposition allows us to decompose it into the product of a lower triangular matrix and its conjugate transpose, i.e.

$$\delta\mathbf{I} + |\mathbf{V}^\delta| = \mathbf{L}\mathbf{L}^*,$$

where $\mathbf{L}$ is a lower triangle matrix with real and positive diagonal entries. This decomposition is unique. Moreover, since

$$0 < \det(\delta\mathbf{I} + \mathbf{V}^\delta) = \det(\mathbf{L})\det(\mathbf{L}^*) = \det(\mathbf{L})\,\overline{\det(\mathbf{L})},$$

it follows that $\mathbf{L}$ is invertible. For each $\alpha > 0$, we have that

$$-\alpha\mathbf{S}_k + \delta\mathbf{I} + |\mathbf{V}^\delta| = -\alpha\mathbf{S}_k + \mathbf{L}\mathbf{L}^* = \mathbf{L}(-\alpha\mathbf{L}^{-1}\mathbf{S}_k(\mathbf{L}^*)^{-1} + \mathbf{I})\mathbf{L}^*.$$

Hence, the positive semi-definiteness of $-\alpha\mathbf{S}_k + \delta\mathbf{I} + |\mathbf{V}^\delta|$ is equivalent to the positive semi-definiteness of $-\alpha\mathbf{L}^{-1}\mathbf{S}_k(\mathbf{L}^*)^{-1} + \mathbf{I}$.

Since both $-\mathbf{L}^{-1}\mathbf{S}_k(\mathbf{L}^*)^{-1}$ and $-\alpha\mathbf{L}^{-1}\mathbf{S}_k(\mathbf{L}^*)^{-1} + \mathbf{I}$ are Hermitian matrices, we can apply Weyl's Inequalities [2, Theorem III.2.1] to obtain

$$\lambda_j(-\alpha\mathbf{L}^{-1}\mathbf{S}_k(\mathbf{L}^*)^{-1} + \mathbf{I}) = \alpha\lambda_j(-\mathbf{L}^{-1}\mathbf{S}_k(\mathbf{L}^*)^{-1}) + 1, \quad j = 1,\ldots,N, \tag{23}$$

where $\lambda_1(\mathbf{A}) \geq \ldots \geq \lambda_N(\mathbf{A})$ denote the N-eigenvalues of some matrix $\mathbf{A}$.

It is known from Lemma 3.5 that $\mathbf{S}_k$ is a positive definite matrix. Thus, the matrix $\mathbf{L}^{-1}\mathbf{S}_k(\mathbf{L}^*)^{-1}$ is positive definite, too. This implies $\lambda_j(-\mathbf{L}^{-1}\mathbf{S}_k(\mathbf{L}^*)^{-1}) < 0$ for all $j = 1,\ldots,N$.

It follows from (23) that for every $j \in \{1,\ldots,n\}$, the functional $\alpha \mapsto \lambda_j(-\alpha\mathbf{L}^{-1}\mathbf{S}_k(\mathbf{L}^*)^{-1} + \mathbf{I})$ is decreasing in α. The biggest α that fulfills

$$\lambda_j(-\alpha\mathbf{L}^{-1}\mathbf{S}_k(\mathbf{L}^*)^{-1} + \mathbf{I}) \geq 0 \quad \text{for all} \quad j = 1,\ldots,N$$

should be

$$\beta_k^\delta = -\frac{1}{\lambda_N(-\mathbf{L}^{-1}\mathbf{S}_k(\mathbf{L}^*)^{-1})},$$

where $\lambda_N(-\mathbf{L}^{-1}\mathbf{S}_k(\mathbf{L}^*)^{-1})$ is the smallest (most negative) eigenvalue of $-\mathbf{L}^{-1}\mathbf{S}_k(\mathbf{L}^*)^{-1}$.

4.3. Minimizing the residual

The minimization problem (18) can be rewritten as follows.

$$\min \left\{ \|\mathbf{V}^\delta + \sum_{k=1}^{P} a_k \mathbf{S}_k\|_F : 0 \leq a_k \leq \min(\mathbf{a}, \beta_k^\delta) \right\}. \tag{24}$$

This problem can be understood as the vector minimization problem if we rearrange the matrix $\mathbf{V}^\delta$ into a long vector and define the N^2-by-P matrix $\mathbf{S}$ whose kth-column stores the matrix $\mathbf{S}_k$:

$$\mathrm{Vec}^\delta_{(i-1)N+j} := (\mathbf{V}^\delta)_{i,j} \quad \text{and} \quad \mathbf{S}_{(i-1)N+j,k} := (\mathbf{S}_k)_{i,j}$$

for $i, j = 1, \ldots, N$ and $k = 1, \ldots, P$. The minimization functional in (24) now becomes

$$\|\mathbf{V}^\delta + \sum_{k=1}^{P} a_k \mathbf{S}_k\|_F^2 = \left\|\mathrm{Vec}^\delta + \mathbf{S}a\right\|_2^2$$

where $a = (a_1, \ldots, a_P)$. Thus, we end up with the following quadratic minimization problem under box constraints:

$$\min \left\{ \|\mathrm{Vec}^\delta + \mathbf{S}a\|_2^2 : \ a_k \in \mathbb{R},\ 0 \leq a_k \leq \min(\mathbf{a}, \beta_k^\delta) \right\}$$

which can be solved, for example, by using the `MATLAB` built-in function `quadprog`. Since the minimization functional $a \mapsto \|\mathrm{Vec}^\delta + \mathbf{S}a\|_2^2$ is convex, every minimizer should be global miminizer.

4.4. Numerical experiments

Figure 1 yields that minimizing the residual under constraint $0 \leq \kappa \leq \sum_{k=1}^{P} \min(\mathbf{a}, \beta_k^\delta)\chi_k$ is not affected much by the noise. Moreover, our method produces no artifacts even under high levels of noise. The upper bound $\mathbf{a}$ is essential not only for preventing infinity bounds when $\beta_k^\delta = \infty$, but also for guaranteeing a good shape reconstruction (figures 1d and 2b). In contrast, the upper bound β_k^δ plays an important role in the proof of the theoretical part, helps to reduce the number of 'admissible' pixels, and makes shape reconstructions slightly better when the noise level is very low (figures 3 and 4).

All of the above arguments hold if we replace the Frobenius norm in (2) by the operator norm. However, the numerical results with respect to the Frobenius norm is much nicer (figures 1d and 2d).

5. Conclusions

We have shown that minimizing the residual of the linearized EIT equation under the constraint $0 \leq \kappa \leq \sum_{k=1}^{P} \min(\mathbf{a}, \beta_k)\chi_k$ yields good approximations to the true conductivity change. The algorithm has real-time implementation, yields no artifacts, and produces good shape reconstructions even under high levels of noise. Moreover, to the best of our knowledge, this is the first reconstruction method based on minimizing the residual which has a rigorous global convergence property. We also expect the same results for the complete electrode model setting.

Acknowledgments

The authors would like to thank Marcel Ullrich, Dominik Garmatter and Janosch Rieger for many fruitful discussions. MNM is also grateful to Li-Chang Hung and Professor Giovanni Alberti for their constant supports.

References

[1] K. Astala and L. Päivärinta. Calderón's inverse conductivity problem in the plane. *Ann. of Math.*, pages 265–299, 2006.

[2] R. Bhatia. Matrix analysis, volume 169 of graduate texts in mathematics, 1997.

[3] A.-P. Calderón. On an inverse boundary value problem. *Soc. Brazil. Mat.*, pages 65–73, 1980.

[4] M. Cheney, D. Isaacson, J. Newell, S. Simske, and J. Goble. Noser: An algorithm for solving the inverse conductivity problem. *International Journal of Imaging Systems and Technology*, 2(2):66–75, 1990.

[5] V. Cherepenin, A. Karpov, A. Korjenevsky, V. Kornienko, A. Mazaletskaya, D. Mazourov, and D. Meister. A 3D electrical impedance tomography (EIT) system for breast cancer detection. *Physiological measurement*, 22(1):9, 2001.

[6] R. G. Douglas. *Banach algebra techniques in operator theory*, volume 179. Springer Science & Business Media, 2012.

[7] I. Frerichs. Electrical impedance tomography (EIT) in applications related to lung and ventilation: a review of experimental and clinical activities. *Physiological measurement*, 21(2):R1, 2000.

[8] B. Gebauer. Localized potentials in electrical impedance tomography. *Inverse Probl. Imaging*, 2:251–269, 2008.

[9] B. Gebauer and N. Hyvönen. Factorization method and irregular inclusions in electrical impedance tomography. *Inverse Problems*, 23:2159–2170, 2007.

[10] B. Harrach. Interpolation of missing electrode data in electrical impedance tomography. *Preprint, available online at www.mathematik.uni-stuttgart.de/oip.*

[11] B. Harrach. Recent progress on the factorization method for electrical impedance tomography. *Computational and mathematical methods in medicine*, 2013.

[12] B. Harrach and J. K. Seo. Exact shape-reconstruction by one-step linearization in electrical impedance tomography. *SIAM Journal on Mathematical Analysis*, 42(4):1505–1518, 2010.

[13] B. Harrach and M. Ullrich. Monotonicity-based shape reconstruction in electrical impedance tomography. *SIAM Journal on Mathematical Analysis*, 45(6):3382–3403, 2013.

[14] A. Kirsch. *An Introduction to the Mathematical Theory of Inverse Problems, Second edition*, volume 120 of *Applied Mathematical Sciences*. Springer Science+Bussiness Media, Springer, 2011.

[15] F. Kittaneh. Inequalities for the Schatten p-norm. iv. *Communications in mathematical physics*, 106(4):581–585, 1986.

[16] R. Kohn and M. Vogelius. Determining Conductivity by Boundary Measurements. *Comm. Pure Appl. Math.*, 37:289–298, 1984.

[17] R. Lazarovitch, D. Rittel, and I. Bucher. Experimental crack identification using electrical impedance tomography. *NDT & E International*, 35(5):301–316, 2002.

[18] A. Lechleiter and A. Rieder. Newton regularizations for impedance tomography: convergence by local injectivity. *Inverse Problems*, 24:065009 (18pp), 2008.

[19] J. L. Mueller and S. Siltanen. *Linear and Nonlinear Inverse Problems with Practical Applications*. SIAM, Philadelphia, 2012.

[20] A. I. Nachman. Global uniqueness for a two-dimensional inverse boundary value problem. *Ann. of Math.*, 143:71–96, 1996.

[21] R. L. Parker. The inverse problem of resistivity sounding. *Geophysics*, 49(12):2143–2158, 1984.

[22] O. Scherzer. *Handbook of Mathematical Methods in Imaging*. Springer Science & Business Media, 2015.

[23] J. Sylvester and G. Uhlmann. A global uniqueness theorem for an inverse boundary value problem. *Ann. of Math.*, 125:153–169, 1987.

[24] A. Tamburrino. Monotonicity based imaging methods for elliptic and parabolic inverse problems. *Journal of Inverse and Ill-posed Problems*, 14(6):633–642, 2006.

[25] N. T. Thanh, L. Beilina, M. V. Klibanov, and M. A. Fiddy. Reconstruction of the refractive index from experimental backscattering data using a globally convergent inverse method. *SIAM Journal on Scientific Computing*, 36(3):B273–B293, 2014.

[26] T. Tidswell, A. Gibson, R. H. Bayford, and D. S. Holder. Three-dimensional electrical impedance tomography of human brain activity. *NeuroImage*, 13(2):283–294, 2001.

[27] N. Young. *An introduction to Hilbert space*. Cambridge university press, 1988.

[28] Q. Y. Zhou, J. Shimada, and A. Sato. Three-dimensional spatial and temporal monitoring of soil water content using electrical resistivity tomography. *Water Resources Research*, 37(2):273–285, 2001.